COMMISSARIAT A L'ENERGIE ATOMIQUE

CENTRE D'ETUDES NUCLEAIRES DE SACLAY
Service de Documentation
F91191 GIF SUR YVETTE CEDEX

CEA-CONF - -9799

L5

SOFT X-RAY AMPLIFICATION IN LASER PLASMAS

LOUIS-JACQUET M.
CEA Centre d'Etudes de Limeil, 94 - Villeneuve-Saint-Georges (FR)

Communication présentée à : International School of Plasma Physics

Varenna (IT)
6-16 Sep 1988

SOFT X-RAY AMPLIFICATION IN LASER PLASMAS

M. LOUIS-JACQUET

C.E.A. LIMEIL-VALENTON
BP 27
94190 VILLENEUVE SAINT-GEORGES
FRANCE

INTRODUCTION

Nearly three decades ago appeared the first visible lasers. Since, important progress have been made involving unnumerable applications in the field of technology as well as in medecine or biology. Rapid development of such lasers was mainly due to the fact that the technique utilized what every physicist finds in his close surroundings. It goes without saying that it would be of considerable interest to produce highly bright sources of shorter wavelengths allowing, for example, the probing of living cells...

Access towards wavelengths covering the far UV or X-UV regions is only available in great laboratories, with synchrotron radiation or emission of hot plasmas. In this paper we will only present a survey (non exhaustive) of soft x-ray amplification produced in laser plasmas which can provide the brightest sources known at the present time.

Historically, the possibility of amplifying a radiation in such plasmas came from the observation of anomalies in the population of specific excited ions existing in the plasma blow-off that could lead to population inversions /1-4/. Because of the short wavelength a major difficulty in x-ray lasers has been the lack of suitable materials for transmission windows and efficient reflectors for resonators which were of high priority in laser research. Consequently, an important effort was done in the search of high gain systems that

would allow substancial amplification.

In this text we shall present in the first section the principle of x-ray amplification in laser plasmas, in the second section the experiments having evidenced such a mechanism, in the third theories and simulations used for modelling, interpretation, and design of targets, and finally we conclude with some actual applications and prospects.

I PRINCIPLES OF SOFT X-RAY AMPLIFICATION AND LASER X

The medium: the laser plasma

In the X-UV wavelength range the photon energy exceeds several tens of eV. So, the corresponding transitions exist in high temperature plasmas composed of highly charged ions. This is easily understandable through the simple Bohr model describing the level energies of an ion of charge Z which are of the order of $Z^2\nu_H$ where ν_H is a frequency of any transition of the hydrogen atom.

The highly charged ions are essentially produced by electron-ion collisions requiring a temperature which is a fraction of Z^2E_H/k where E_H is the ionization potential of hydrogen. In plasmas created by interaction of a powerful laser beam with a solid target it is usual to define three zones of different temperature and density (Fig 1): a compressed one inside the solid where the plasma is in LTE,

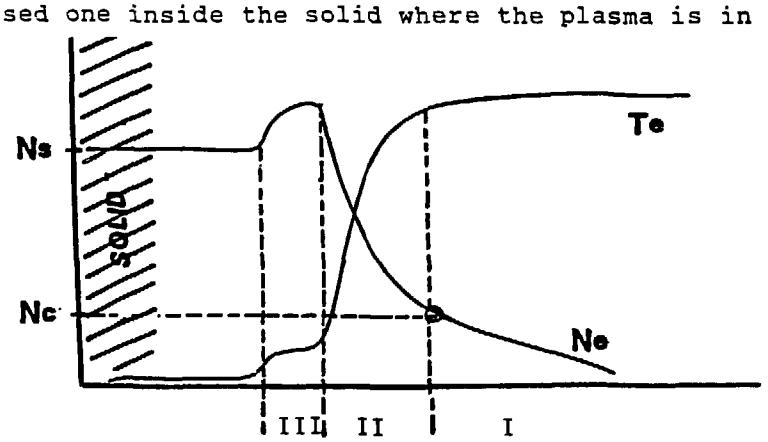

Fig 1: Scheme of density and temperature profiles in a laser plasma. Corona (I); conduction zone (II); compressed zone (III).

then a conduction zone where temperature and density gradients are steep, and an expansion zone with quasi-uniform temperature and low density. The last two zones are more or less in strong non-LTE implying probable population inversions where values of Te and Ne are typically 10^6 - 10^7 K and 10^{19} - 10^{21} e^-/cm^3.

Definition of the gain

Every time the following question is formulated: "how can be amplified a particular mechanism?", one always refers to Einstein coefficients, and for photons the answer is found through the transfer equation:

$$\frac{\partial I_\nu}{c\partial t} + \vec{\nabla} I_\nu . \vec{\Omega} = j_\nu - k_\nu$$

where I_ν is the light intensity at a given frequency ν, j_ν and k_ν the emission and absorption coefficients, and $\vec{\Omega}$ the unit vector in the direction of the light propagation. If k_ν is negative the medium is an amplificator. For the ideal case where the first term of the equation can be neglected and the medium is considered as uniform the solution is:

$$I_\nu(x) = (I_\nu(0) - j_\nu/k_\nu)\exp(-k_\nu x) + j_\nu/k_\nu$$

For a bound-bound transition and the complete frequency redistribution $\phi_{sp\ em} = \phi_{in\ em} = \phi_{abs}$ (ϕ is the line profile), the gain coefficient $\alpha_\nu = -k_\nu$ is expressed as:

$$\alpha_\nu = -k_\nu = c^2/8\pi\nu^2 A_{ul}\phi\, g_l(n_u/g_l - n_u/g_u)$$

and the source function:

$$j_\nu/k_\nu = 2h\nu^3/c^2/(g_u n_l/(g_l n_u) - 1)$$

where A_{ul} is the spontaneous emission coefficient, n and g the densities and statistical weights of the upper and lower discrete states. Amplification occurs when the condition for inversion population is satisfied, ie:

$$n_u/g_l - n_l/g_u > 0$$

If no outer photon enters the medium (I (0)=0), amplification of spontaneous emission (ASE) takes place.

Population inversion

To achieve population inversions, electrons and photons can independantly play a fundamental role. The recombination of an electron to an ion was proposed in 1970 by Gudzenko and Shelepin as a possible mechanism of inversion. In Fig 2a the upper levels are populated by recombination of electrons and the lower levels rapidly depopulated by radiative decay. In the collisional excitation process the earliest paper was published by Molchanov /5/. The principle for Ne-like ions is explained in Fig 2b: the upper level 3d is populated by collisional excitation from the fundamental 2p and can be depopulated only towards the 3p because of the selection rules, giving rise to an inversion beetwen the 3p and the 3s.

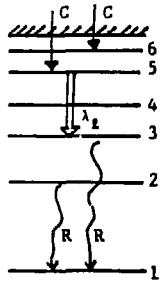

a: recombination

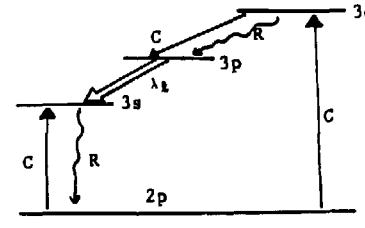

b: collisional excitation

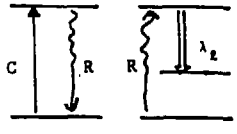

c: resonant photoexcitation

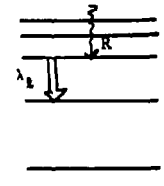

d: photoionization

Fig 2: inversion schemes

The use of optical pumping with a resonant radiation is well known and the first published proposal in the soft x-rays is that of Vinogradov /6/. A strong line emitted by a specific ion might be used to actively pump a x-ray transition of a ion of different species (Fig 2c). The main issue of this scheme is the difficult matching of both wavelengths and consequently the adjustment of the profiles of the pump line and the line corresponding to the absorbing transition. The inversion produced by photoionization was well describe by Duguay and Rentzepis /7/. The idea is to remove inner-shell electrons selectively from ions which have lost a small number of electrons through another mechanisms; the resulting population can be inverted against radiative transitions filling the inner shell hole (Fig 2d).

Saturation

When the amplified radiation becomes intense it strongly repopulates the upper level of the lasing transition, so that the gain is not as high as expected. The maximum gain is then deduced by equating the stimulated rate to the total exit rate from the upper state.

Superradiance

In the objective of creating a x-ray laser, the ions emitting the lasing transition have to radiate in a cooperative manner: such a process is call superradiance. It can occur above a threshold of density of excited ions. When this is realized few modes only can propagate in the medium. Suppose N active ions in the plasma of length L, two ions are undistinguisable if the inter-ion distance is smaller than the transition wavelength λ: hence,

$$N\lambda / L >> 1.$$

This condition is equivalent to :

$$t_{sr} = L/(N\lambda A_{ul}) << 1/ A_{ul} ,$$

where t_{sr} is a characteritic time of superradiance. Another one is the time necessary to reach the maximum of

intensity. In fact dephasing effects can hinder the development of the cooperative emission of photons, such that the above threshold may be replaced by $t_{sr} << t^*$ where t^* is the relaxation time of the upper level which take into account the ion motion. From this condition one can deduce a minimum value of the gain-length (15) product to achieve superradiance and then a x-ray laser.

II EXPERIMENTS

The first positive experimental results who claimed an amplification in the far UV range were published in the early 1970s. But evidence of strong x-ray amplification was only given four years ago. In the following we shall describe the outstanding experiments the results of which have been explained through the two main recombination and collisionnal excitation inversion schemes.

In all experiments the medium must be as long as possible in order to obtain at once a detectable amplification and a plasma in optimal conditions that produce an efficient population inversion. Such an elongated plasma is most often created by focusing the driven laser beam with a set of optics having a strong astigmatism (tilted mirrors or cylindrical lenses).

Recombination experiments

As previously mentionned this scheme works all the more as the plasma is rapidly cooled. Two ways have been successively used: the first is to shoot on a target and let the plasma expand freely in the vacuum /8/. Amplification was observed in the 5f-3d (λ=106Å) of Li-like ions of Al. The weak gain (1/cm) was inferred by varying the plasma length in successive shots (Figs 3-4). The incoming laser characteristics were λ_L=1.06μm, τ_L=1ns, $I_L=10^{10}W/cm^2$.

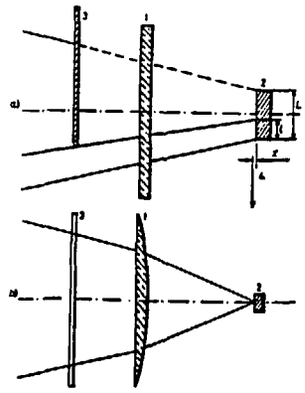

– Simplified sketch of the experimental arrangement used for producing plasma columns of various lengths with a constant flux density on the target. a) and b) are, respectively, the horizontal and the vertical cross-section: 1) cylindrical lens (for simplicity, the spherical lens is not represented), 2) aluminium target, 3) adjustable shield whose position determines the length of the plasma line, 4) observation axis provided with a spatial resolution system followed by a grazing incidence grating and either an optical multichannel analyser (time-integrated measurements) or a streak camera (time-resolved measurements); this axis is in the horizontal symmetry plan, at short distance X from target surface.

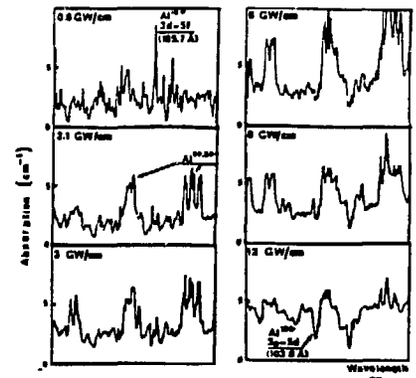

Experimental time-integrated absorption spectra of aluminum plasma, between 100 and 110 Å, for a set of increasing laser flux densities. After giving rise to a strong absorbing line at a flux density (0.8 GW/cm), the 5f–3d transition turns to supply a negative contribution to background absorption at high flux. Laser pulse duration, 3.5 nsec.

Fig 3 Fig 4

In the same way the recombination of a carbon plasma from bare nucleus to hydrogenic ion has been extensively studied. Figs 5-6 show the experimental set-up and results obtained with a carbon fiber target (up to 1 cm long and few μm in diameter)/9/. The fiber was irradiated with the caustic of a mirror used under grazing incidence. The Nd laser (λ_L=0.53 μm) delivered few tens J in 70ps. Because of the small radius of the fiber the plasma expands rapidly in an adiabatic cooling inducing a strong decrease in temperature and avoids also the reabsorption of radiations that might populate the lower level of the lasing transition. Gains measured in the 3p-2s transition (182Å) was about 4/cm.

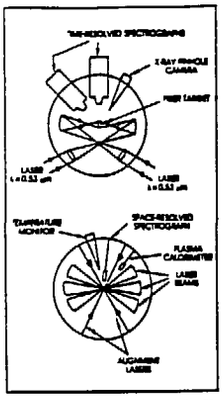

In this experimental target chamber arrangement used for short-wavelength x-ray laser studies at Rutherford Appleton Laboratory, Oxfordshire, U.K., six beams from the Nd:glass laser Vulcan are brought to a common line focus using the aberration of spherical mirrors.

Fig 5

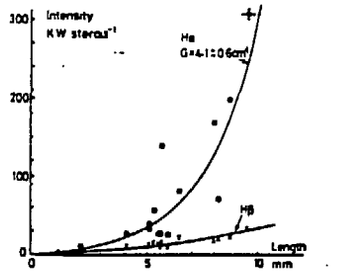

• Ordinate: absolute intensity of axial H_α and H_β emissions measured from streaked spectra 975 psec after the peak of the laser pulse. Abscissa: irradiated length. A typical measurement error bar is shown for H_α. Theoretical fits to the experimental data are also plotted.

Fig 6

A different approach has been used /10/ with the irradiation of a carbon target by a CO_2 laser (500J,50ns, 10.6μm), (Fig 7). The plasma is confined by an axial magnetic field and its cooling is caused to thermal radiation which seems better than adiabatic cooling in free expansion. Fig 8 shows experimental results of gain in the Balmer α (182Å), deduced from measurements of axial and longitudinal spectra.

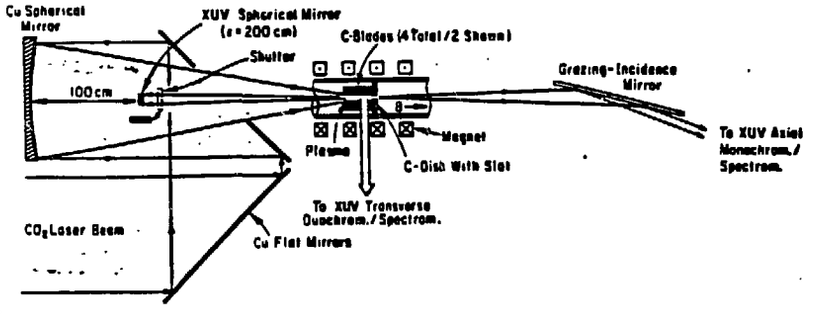

Experimental setup with xuv spherical mirror.

Fig 7

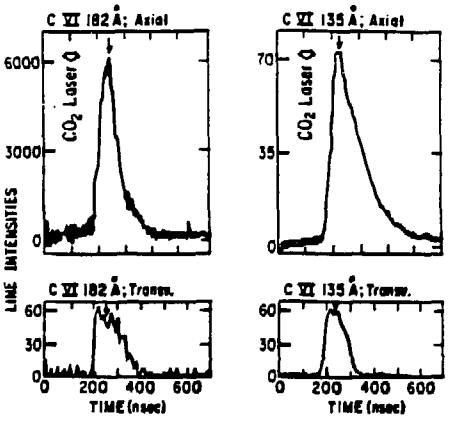

Time evolution of C VI 182-Å and 135-Å line intensities measured with axial and transverse xuv instruments for two discharges with the same plasma conditions. The enhancement for the 182-Å line was $E \approx 100$; the one-pass gain was $kl = 6.5$.

Fig 8

Collisional excitation experiments

The first strong amplification /11/ was observed in the 3p-3s transitions of Ne-like ions of selenium. The target composed of a thin layer (750 A) of Se deposited on a Formvar substrate (1000 A) was irradiated on both sides at 4 10^{13} W/cm^2 with 0.53 m light during 0.5 ns. Fig 9 show the experimental set-up , Fig 10 a spectrum in the soft x-ray range where we can see the main amplified lines, and a curve of the intensities of the J=2-1 lines at 206 and 209 A versus the length of the medium, which was varied up to 5 cm. Gains of about 6/cm were found.

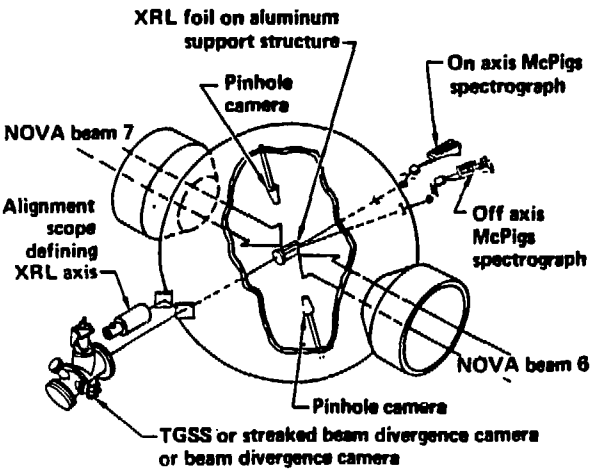

Fig 9

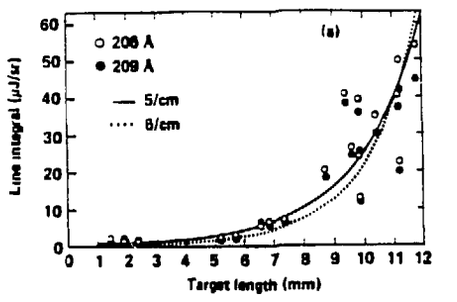

Integrated line intensity of $J=2$ to 1 transitions vs amplifier length

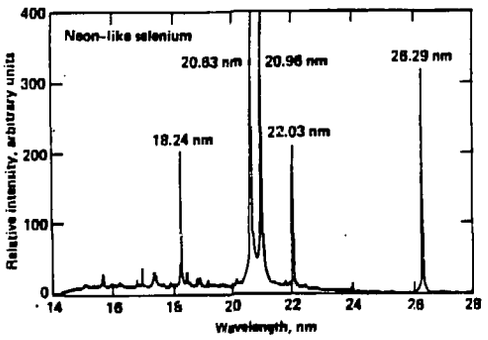

Fig 10

With a Nd driving laser working at its fundamental wavelength λ_L=1.06 μm, and a pulse duration of 2 ns, amplification has been measured for the same transitions as above in Ne-like ions of Ge /12/. Figs 11 and 12 experimental set-up and spectra.

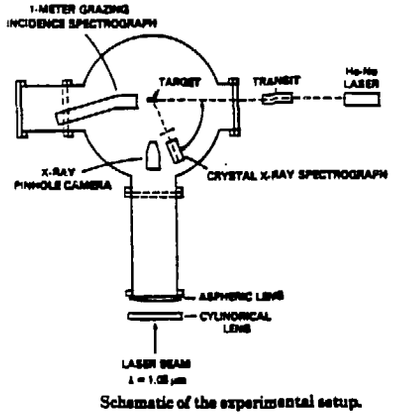

Schematic of the experimental setup.

Fig 11

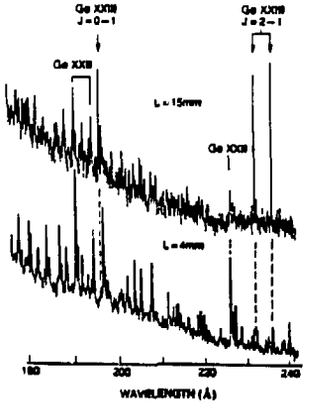

Microdensitometer traces of second-order spectra obtained for plasma lengths of 4 and 15 mm, showing the neonlike Ge XXIII (Ge^{22+} ion) lasing lines at 236.26 and 232.24 Å ($J=2$ to 1) and 196.06 Å ($J=0$ to 1) increasing with length. Sodiumlike Ge XXII lines shown arise from 3→3 transitions.

Fig12

In the same way and at the same time gain results were obtained at CEL-V /13/ with thin foils of Ge and similar laser characteristics (except the pulse duration 1 ns), Fig 13.

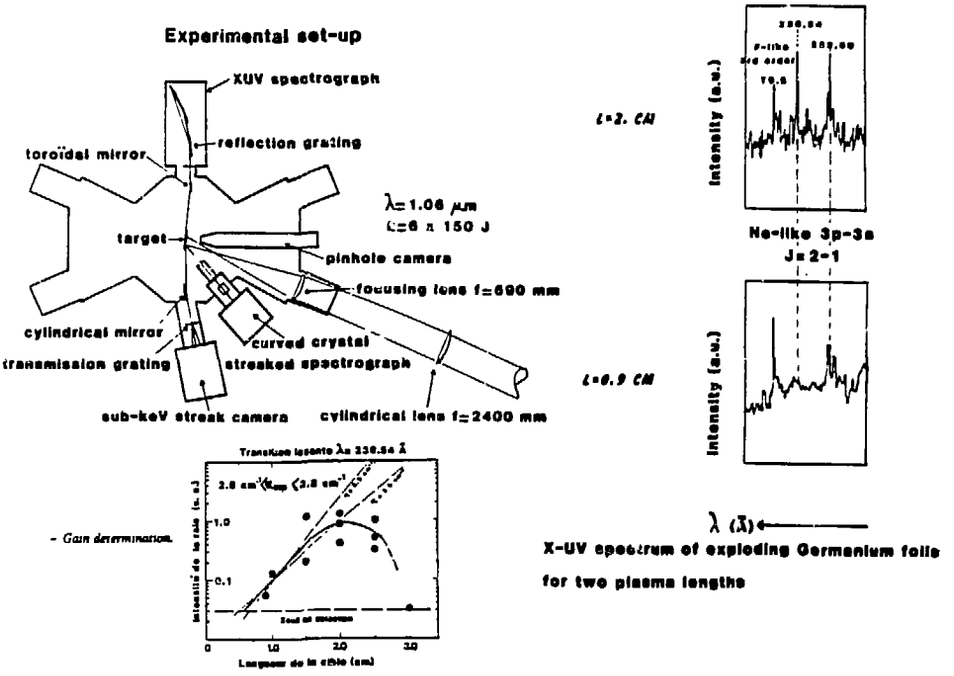

Fig 13

We must notice the decreasing of the intensity of the amplified line when the target is very long. For the actual experiment this is due to the combined effects of refraction of the radiation in plasma gradients and the too small field of the spectrograph that records the spectra.

Still at CEL-V, we performed experiments with the powerful Phebus laser working at the 0.53 and 0.35 μm lights, with the idea to optimize the amplification in Ne-like ion systems by varying both nature and thickness of targets and laser irradiation. In Fig 14 we find two spectra recorded for two plasma lengths at a time corresponding to the maximum intensity of the amplified lines. From preliminary analysis it comes out that Se seems to be a good candidate and 0.53 μm is better than 0.35 μm light for irradiating the targets because of plasma non-uniformities that appear with the 0.35 μm light preventing

the amplification to grow. To date the most intense x-ray source has been obtained with Se target foils delivering about 1 mJ at λ=200 Å during 200 ps.

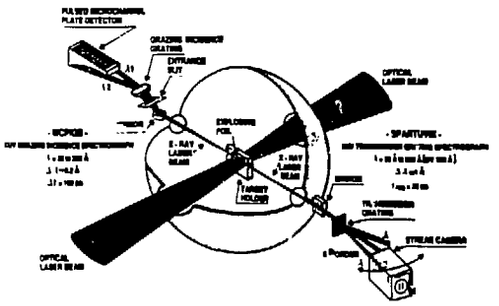

:X-ray laser experimental set-up at Phebus laser facility

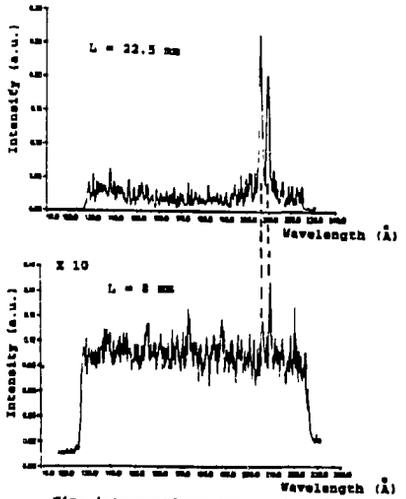

:Time integrated spectra for two plasma lengths showing the neon like Selenium lasing lines at 206.3 Å and 209.6 Å (J=2-1)

Fig 14

In the intent to qualify both the x-ray radiation and the plasma characteristics, important work has been done in the field of x-ray diagnostics. So, we applied new performing technologies to develop two specific x-ray spectrographs providing high time resolution (30 ps) by the use of x-ray streak cameras as detectors, and spectral resolution by means of either transmission gratings (5000 Å period) /14/ or curved crystals (TlAp, PET) for the X-UV (λ=20-300 A, $\Delta\lambda$=1 Å) and X (λ = 4.5-12 A, $\Delta\lambda$ = 2 10-2 Å) wavelength ranges respectively, see Fig 15,16.

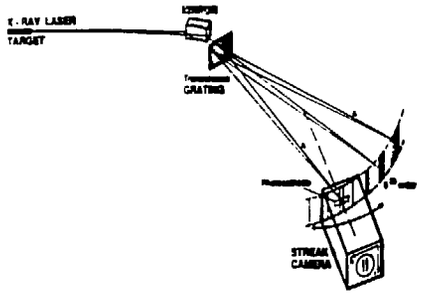

Schematic of the time resolving X-UV transmission grating spectrograph

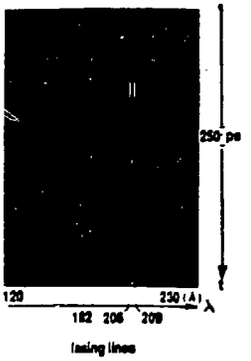

Time resolved spectrum of the 3s-3p lines of Ne-like ions of Selenium

Fig 14

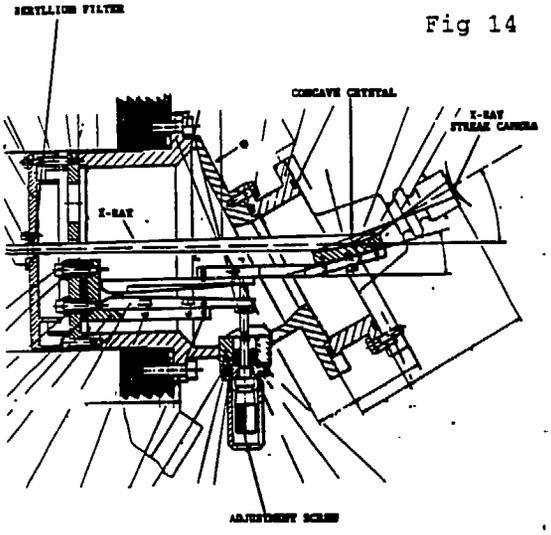

Schematic of the time resolving x-ray curved crystal spectrograph

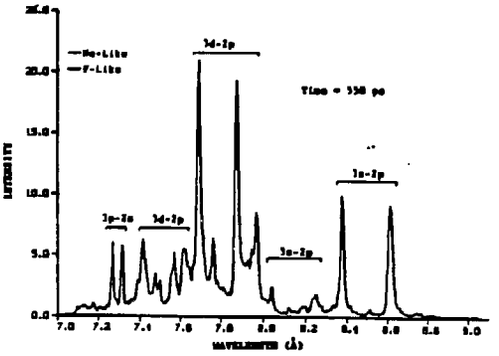

Line-out of the 3-2 Se^{24+} spectrum at a given time

Fig 15

THEORY AND SIMULATION

The most general way to design and interpret x-ray laser experiments is a complete physical simulation Fig 16. Such a simulation is performed in several steps. First, a hydrodynamic lagrangian code gives electron temperature and density as functions of time in each cell taking into account absorption processes of the laser light which creates the plasma, energy and radiation transfers

including non-LTE ionization mechanisms. The second step is the use of a kinetic code as a post-processor of the first code which provides the populations of excited states and the ionic abundances as functions of time and space. Processes taken into account are collisional ionization, auto-ionization, photoionization, collisional excitation, photo excitaion, and for each, the inverse process. To reduce too large computer times a steady state approximation of the fully time dependant calculation can be used if permitted. Knowing all the populations, gains of transitions in corn are easily determined. The last step is the integration of the transfer equation of the different radiations the intensities of which are recorded with the set of spectrographs described in section II, and compared to experimental results.

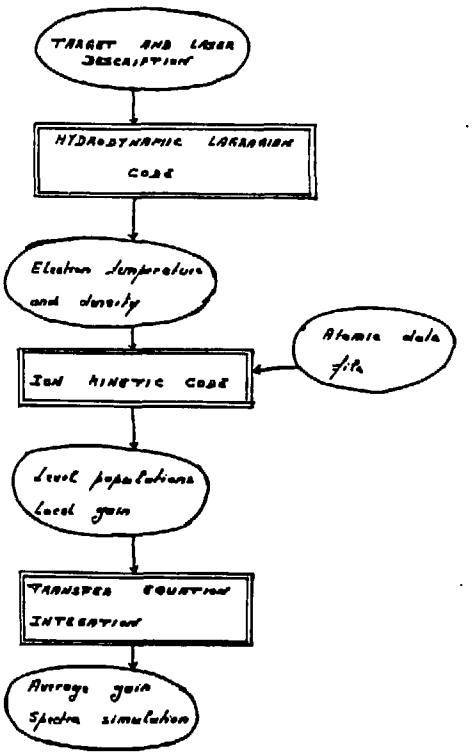

Fig 16

For example, Figs 17,18 show spatial profiles of temperature and density at different times for a thin foil of Ge irradiated on both sides at 5 10^{12}W/cm^2 with 1.06 μm light.

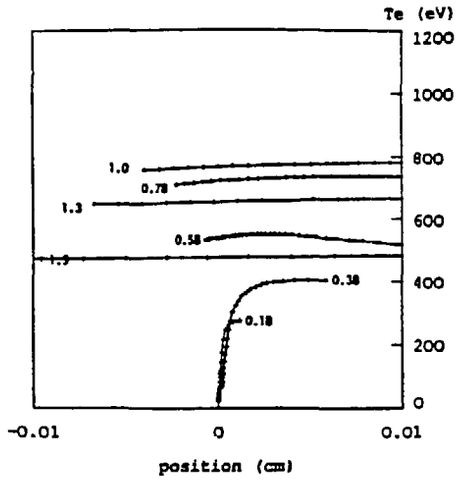

Fig 17

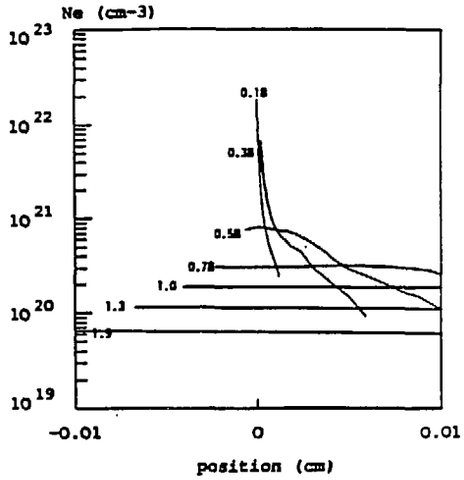

Fig 18

For the second step of calculation we need a good description of atomic physics of ion species that populate the plasma. Fig 19 gives an idea of the complexity of

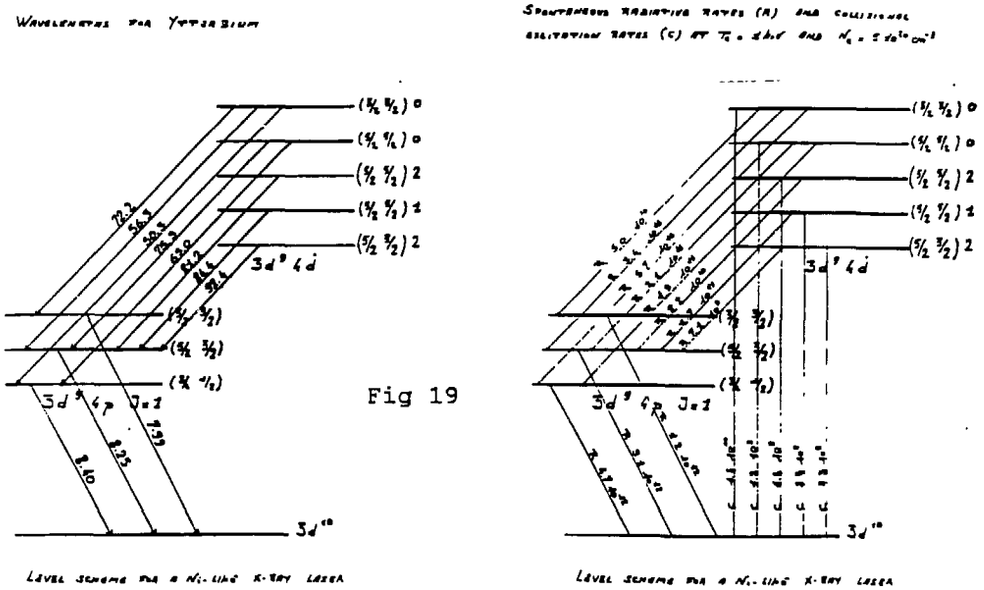

Fig 19

levels for a Ni-like ion of Ytterbium and some values of collisonal and radiative rates which have to be precisely calculated to understand the relative importance of the different processes. The large excitation cross section of the $3d^{10}$-$3d^{9}4d$ (J=0) and the large decay rates 3d94p (J=1)-$3d^{10}$ provide the population inversion between 3d94d and $3d^{9}4p$. For Ni-like ions, numerical simulations correctly reproduce the gain in various lines, Fig 20, but for Ne-like ions the J=0-1 transition has a theoretical gain much larger than the measured value.

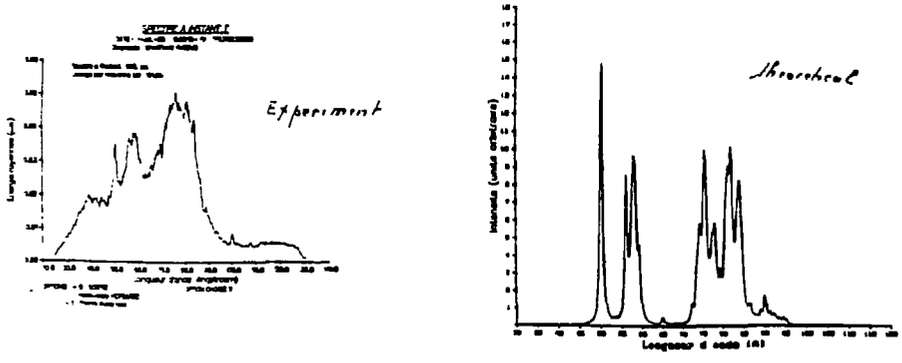

Fig 20

To design targets and laser used for performing an experiment an accurate simple model of hydrodynamics of exploding foils have been developed /15/. The model predicts the conditions in the foil plasma for given experimental parameters. It is based on an isothermal, homogeneous expansion similarity solution of the ideal hydrodynamic equation. Very useful scaling laws are deduced. On another hand a code using kinetic equation of ion population has been developed that allows the determination of plasma parameters /16/, temperature and density gradients by comparison of theoretical and experimental line intensity ratios, Fig 21.

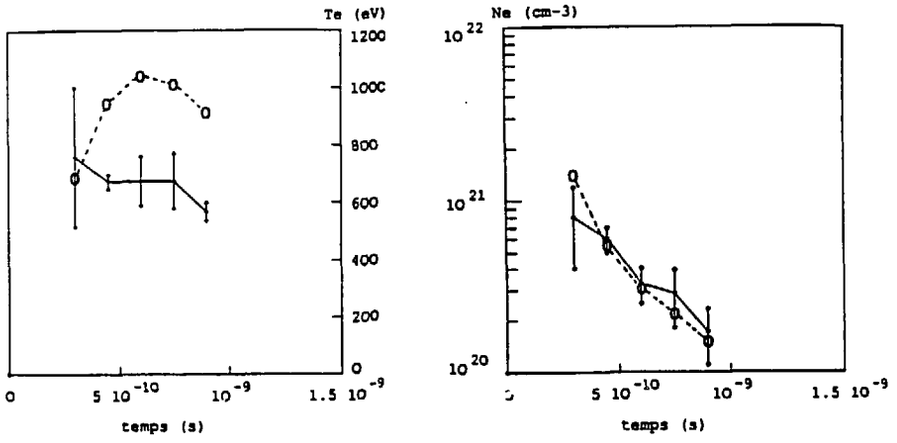

Fig 21

APPLICATIONS AND PROSPECTS

In the following we shall examine some applications which can use the intense x-ray source already produced with target working in the collisional excitation scheme /17/.

Grating production

Two types of grating production techniques are potentially possible with x-ray lasers :spatial period division and holography. In spatial period division the near field diffraction pattern of a parent transmission grating is used to produce a fringe pattern with a spatial period at harmonics of the parent grating period. The illuminating light source does not to be coherent. It is only necessary to be monochromatic and intense. Current x-ray laser meet these requirements. A possible arrangement for producing transmission grating using a soft x-ray laser is given in Fig 22. The output is focused by a spherical multi-layer mirror down to a 1mm diameter spot. With a 2000 A parent grating both 1000 and 667 A gratings should be possible.

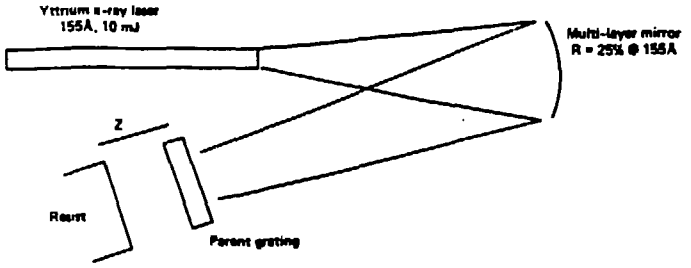

Schematic arrangement for using the yttrium x-ray laser in spatial period divison for grating production.

Fig 22

It is possible to consider using the x-ray laser to produce reflection gratings holographically. Here the x-ray beam is split into two beams. They are then recombined at the photoresist producing an interference pattern.

Contact microscopy

Contact microscopy offers the possibility of near term biological applications of x-ray lasers. In contact microscopy a sample to be analyzed is placed on photoresist and exposed to incident x-rays. The resist is then developed and opacity map of the sample is obtained.This opacity map on the photoresist is then scanned by an electron microscope.X-ray laser is sufficiently bright for this type of microscopy and there is no need for coherence. By exposing a sample to a single wavelength, the distribution of the highly absorbing stain can be mapped yielding structural information. A possible arrangement for performing contact microscopy using a yttrium laser is shown in Fig 23. The laser is focused by multilayer mirror to a spot ,and acts like a bandpass filter. The sample is placed behind the vaccum window on PMMA resist. With a 5 mrad divergence laser and 1 μm thick sample, the resolution would be about 1000 - 2000 Å. Since the transmission of the water and protein at 155 Å is extremely low, the sample would have to be dehydrated.

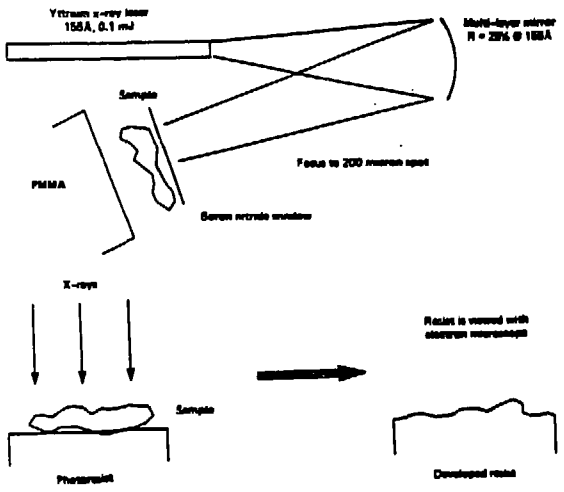

Contact microscopy with the yttrium laser.

Fig 23

Holography /18/

X-ray holography offers the potential for obtaining high-resolution three-dimensional images of in vitro biological microstructures. Significant progress toward this goal has been achieved with holography systems using synchrotron x-ray sources. The experiments required x-ray exposures of an hour or longer, which makes high spatial resolution difficult to achieve in live biological specimens because of blurring of the image,caused by specimen motion. A possible solution to this problem is to exploit the high brightness and coherence lengths produced by x-ray lasers; the hologram could then be made with exposure times of less than 1 nsec.The holography geometry used was a Gabor in-line type modifed by the inclusion of a high reflectivity multilayer x-ray mirror used as a norrow bandpass filter, as shown in Fig 24. The longitudinal coherence length of the laser emission is estimated to be greater than 100 μm. the lower bound on transverse coherence length is 3.5 μm at the end of the x-ray laser amplifier. The spatial resolution of the holography system can be estimated from the resolution limits for Gabor

holography to be approximately 5 μm with the dominant limitation being the film spatial resolution.

With laser wavelength in the water window (4.4 to 2.3 nm) where there is high contrast between protein and water, x-ray holograms of living cells can be produced.

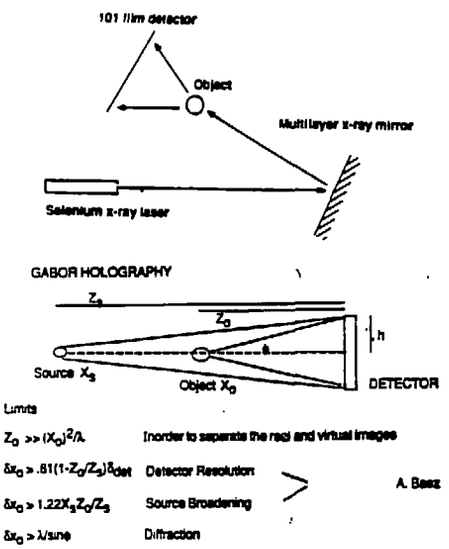

Schematic arrangement of the Gabor in-line holography geometry modified by the inclusion of a narrow bandpass multilayer x-ray mirror.

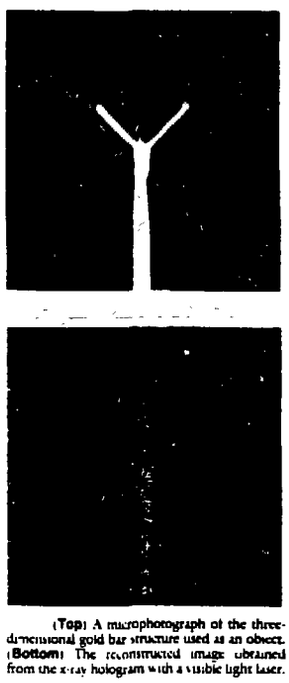

(Top) A microphotograph of the three-dimensional gold bar structure used as an object. (Bottom) The reconstructed image obtained from the x-ray hologram with a visible light laser.

Fig 24

Intense coherent line sources of x-rays are of great importance in atomic physics experiments. They can be used as radiative pumps of short pulse duration to ionize or excite inner shells of neutral atoms and ions for studying radiative cascades and determining oscillator strengths of particular transitions.

As a conclusion one can say that the way to the feasability of an x-ray laser is really open and there is an amount of possible applications. A new attemp is now to deacrease the wavelength with a minimum in power investment by choosing the best candidate, inversion scheme, and wavelength of the driving laser.

/1/ F.E. Irons, N.J. Peacock
J. Phys B, 7, 1109, 1974
/2/ V.A. Bhagavatula, B. Yaakobi
Optics Communications 24, 331, 1978
/3/ P. Jaegle et al.
Physics Letters 36A, 30, 1971
/4/ G.J. Pert
J. Phys B, 9, 3301,1976
/5/ A.G. Molchanov
Sov. Phys. Usp. 15, 124, 1972
/6/ A.V. Vinogradov, I.I. Sobelman,E.A. Yukov
Sov. J. Quant. Elect. 5, 9, 1975
/7/ M.A. Duguay, P.M. Rentzepis
Appl. Phys. Letters 10, 350, 1967
/8/ P. Jaegle et al
J.O.S.A B, 4, 563, 1987
/9/ C. Chenais-Popovics et al
Phys. Rev. Lett. 59, 2161, 1987
/10/S. Suckewer et al
Phys. Rev. Lett. 55, 1753, 1985
/11/D.L. Matthews et al
Phys. Rev. Lett. 54, 110, 1985
/12/T.N. Lee et al
Phys. Rev. Lett. 59, 1185, 1987
/13/M. Louis-Jacquet et al
C. R. Acad. Sci. Paris 306, 867, 1988
/14/J-L. Bourgade et al
to be published in Rev. Sci. Instruments
/15/R.A. London and M.D. Rosen
Phys. Fuids 29, 3813, 1986
/16/O. Peyrusse et al
to be pulished in J. of Appl. Physics
/17/J.E. Trebes
Journal de Physique C6, 10, 47, 309, 1986
/18/J.E. Trebes et al
Science 238, 517, 1987